Original Paper

Cellular Physiology and Biochemistry

Cell Physiol Biochem 2010;26:749-760

Accepted: September 23, 2010

Acid Sphingomyelinase Deficiency Attenuates Bleomycin-Induced Lung Inflammation and Fibrosis in Mice

Rajwinder Dhami, Xingxuan He and Edward H. Schuchman

Department of Genetics & Genomic Sciences, Mount Sinai School of Medicine, New York

Key Words
Sphingolipids • Signal transduction • Cell growth • Fibrosis

Abstract
Background/Aims: The sphingomyelin/ceramide signaling pathway is an important component of many cellular processes implicated in the pathogenesis of lung disease. Acid sphingomyelinase (ASM) is a key mediator of this pathway, but its specific role in pulmonary fibrosis has not been previously investigated. Here we used the bleomycin model of pulmonary fibrosis to investigate fibrotic responses in normal and ASM knockout ($ASM^{-/-}$) mice, and in NIH3T3 fibroblasts with and without ASM siRNA treatment. Methods: Mice and cells with and without ASM activity were treated with bleomycin, and the effects on lung inflammation, formation of collagen producing myofibroblasts, and apoptosis were assessed. Results: The development of bleomycin-induced inflammation and fibrosis in wildtype mice correlated with the rapid activation of ASM, and was markedly attenuated in the absence of ASM activity. Along with the elevated ASM activity, there also was an elevation of acid ceramidase (AC) activity, which was sustained for up to 14 days post-bleomycin treatment. Studies in NIH3T3 fibroblasts confirmed these findings, and revealed a direct effect of ASM/AC activation on the formation of myofibroblasts. Cell studies also showed that a downstream effect of bleomycin treatment was the production of sphingosine-1-phosphate. Conclusions: These data demonstrate that the sphingomyelin/ceramide signaling pathway is involved in the pathogenesis of bleomycin-induced pulmonary fibrosis, and suggest that inhibition of ASM may potentially slow the fibrotic process in the lung.

Copyright © 2010 S. Karger AG, Basel

Introduction

Idiopathic pulmonary fibrosis (IPF) is a progressive, interstitial lung disease with a post-diagnosis median survival rate of only 2 to 3 years [1-3]. It is characterized by abnormal lung architecture resulting from excessive extracellular matrix (ECM) deposition and accompanying inflammation of varying degrees. Successful therapies are lacking for this disorder. The pathogenesis of IPF has been actively studied, but specific mechanisms leading to the disease remain elusive. Historically, chronic

KARGER
Fax +41 61 306 12 34
E-Mail karger@karger.ch
www.karger.com

© 2010 S. Karger AG, Basel
1015-8987/10/0265-0749$26.00/0

Accessible online at:
www.karger.com/cpb

Edward H. Schuchman, PhD
Genetic Disease Foundation – Francis Crick Professor,
Dept Genet & Genom Sci, Mount Sinai School of Medicine
1425 Madison Avenue, Room 14-20A, New York, NY 10029 (USA)
Tel. +12126596711, Fax +12128492447, E-Mail Edward.schuchman@mssm.edu

inflammation, and more recently, aberrant wound healing and epithelial/mesenchymal crosstalk, are believed to be significant components of the pathogenic process [4]. The formation of fibroblastic foci resulting from hyperproliferation of alveolar epithelial cells, as well as a local increase in collagen-producing fibroblasts, are key components contributing to the disease progression. The fibroblasts responsible for ECM reorganization are referred to as myofibroblasts [5, 6], and understanding the pathways leading to their proliferation, differentiation and activation is essential for developing novel therapeutic approaches for the treatment of pulmonary fibrosis.

Acid sphingomyelinase (ASM, E.C. 3.1.4.12) is the lysosomal enzyme responsible for the hydrolysis of sphingomyelin, resulting in the production of ceramide, a bioactive lipid that has been implicated in the pathogenesis of numerous human diseases, including cancer, atherosclerosis, diabetes, emphysema, cystic fibrosis and others [7, 8]. An inherited deficiency of ASM activity results in the type A and B forms of Niemann-Pick disease (MIM# 257200). In addition to its housekeeping function in lysosomes, ASM activation occurs in response to many extrinsic stress factors and/or specific developmental cues, and results in the rapid generation of ceramide within the plasma membrane. This, in turn, results in reorganization of membrane microdomains, which activates signaling pathways that usually lead to apoptosis [9, 10]. Importantly, ASM exists in a complex with another enzyme of sphingolipid metabolism, acid ceramidase (AC; E.C. 3.5.1.23) [11]. Acid ceramidase can hydrolyze ceramide, producing sphingosine and ultimately sphingosine-1-phosphate (S1P), another important bioactive lipid and a recognized mediator of cell survival, proliferation and differentiation [12].

Although the role of sphingolipid signaling, and ASM specifically, in IPF has not been studied, a substantial and relevant literature has recently emerged in cystic fibrosis, where mouse models have been shown to have elevated ceramide in their lungs, correlating with the age-related progression of inflammation and fibrosis [13, 14]. ASM appears to be a key mediator of this pathway, and genetic or pharmacologic inhibition of ASM in cystic fibrosis mice blocks excessive ceramide production in their lungs and corrects pathological findings. Indeed, the first reports of ASM inhibition have recently been published in cystic fibrosis patients, where improved lung function was observed [15]. In addition to these findings, ASM also has been recently implicated in the etiology of liver fibrosis, where the selective overexpression of this enzyme has been shown to occur during the transdifferentiation/ activation of primary mouse hepatic stellate cells into myofibroblast-like cells [16]. Finally, consistent with these findings, early studies from our laboratory showed that mice lacking ASM (i.e., ASM knockout; $ASM^{-/-}$ mice) exhibited little or no evidence of lung fibrosis, despite considerable age-progressive inflammation in their lungs [17, 18].

Thus, these data suggest that ASM is an important component of the fibrotic process. In this manuscript we investigate this hypothesis further by employing a common animal model of lung fibrosis, the bleomycin-mediated mouse model [19-22]. Bleomycin is an effective chemotherapy drug, although its clinical utility is limited due to the development of pulmonary fibrosis. Based on this observation, bleomycin is frequently used in experimental animals to induce pulmonary fibrosis. Although lacking some important features of human fibrosis, the bleomycin-mediated mouse model demonstrates significant features of human IPF, including a marked inflammatory response accompanied by epithelial cell injury, basement membrane damage, and interstitial as well as intra-alveolar fibrosis. Other methods to produce pulmonary fibrosis in animal models have been investigated, but bleomycin remains the most efficient, reproducible, and widely used.

Materials and Methods

Reagents and kits

Bleomycin sulfate and the Accustain Trichrome Kit were purchased from Sigma Aldrich (St. Louis, MO). Polyclonal alpha-smooth muscle actin (alpha-SMA) antibody for immunolabeling was purchased from LabVision (Fremont, CA). Dulbecco's Modified Eagle's Medium (DMEM) was from Fisher Scientific (Pittsburgh, PA). Anti-Rabbit Vectastain ABC and DAB Substrate Kits were purchased from Vector Labs (Burlingame, CA). The Deadend Colorimetric TUNEL System was purchased from Promega (Madison, WI). The Sircol Collagen Assay Kit was from Accurate Chemical and Scientific Corp. (Westbury, NY). The mouse embryonic fibroblast cell line, NIH3T3 (Cat. No. CRL 1658), was purchased from American Type Culture Collection (Manassas, VA). Naphthalene-2,3-dicarboxaldehyde (NDA) was purchased from Molecular Probes (Eugene, OR). Sodium cyanide was from ICN Biomedical (Aurora, OH). D-erythro-sphingosine-1-phosphate was from Avanti Polar Lipids (Alabaster, AL). All other biochemical reagents, including Igepal CA-630, were from the Sigma Aldrich.

Mice and bleomycin treatment

ASM null mice ($ASM^{-/-}$) [17] were bred in the C57BL/6J background. Eight-10 week old wildtype C57BL/6J and age- and sex-matched $ASM^{-/-}$ mice were used. Mice were treated

with either saline or 50 µg (0.1 units) of bleomycin sulfate in saline by intratracheal injection in a total volume of 50 µl. This protocol has been used by others and shown to produce substantial inflammation and fibrosis in normal mice [3, 21]. Animals were sacrificed for analysis after 2, 7, 14, or 28 days. The experimental protocol was approved by the Mount Sinai School of Medicine Institutional Animal Care and Utilization Committee. All animal studies were conducted in accordance with the Guide for the Care and Use of Laboratory Animals, as adopted by the U.S. National Institutes of Health.

Histology and immunohistochemistry

Paraffin-embedded lung sections were prepared and stained as previously described [18]. The trichrome staining kit for collagen was used according to the manufacturer's instructions. For alpha-SMA immunolabeling, sections were incubated for 1.5 hours at room temperature with ready-to-use antibody (LabVision), followed by treatment with the Anti-Rabbit Vectastain ABC and DAB Substrate Kits as per the manufacturer's instructions.

Detection of apoptosis in lung sections

Apoptotic cells were detected in formalin-fixed, paraffin-embedded lung sections using the Deadend Colorimetric TUNEL System as per the manufacturer's instructions. Immuno-positive cells were counted in 5 random fields of view for each lung section under 20X magnification.

Quantification of enzyme activities

Fluorescence-based, high performance liquid chromatographic (HPLC) methods were used to measure ASM and AC activities in total lung and cell lysates as previously described [23, 24].

Quantification of ceramide

Ceramide was quantified in total lung lysates using a modification of the diacylglycerol kinase assay [25]. 10 µl of lung tissue homogenates were heated at 70ºC for 5 minutes, cooled to room temperature and briefly centrifuged. Two microliters was then mixed with 8 µl of a solution containing 7.5% n-octyl-b-D-glucopyranoside, 5 mM cadiolipin, and 1 mM DETAPAC. This was added to 30 µl of a buffered solution containing 0.1 M imidazole-HCl, pH 6.6, 0.1 M NaCl, 25 mM MgCl2, 4 mM DTT, and 2 mM EGTA. Five microliters of enzyme buffer (10 mM imidazole-HCl, pH 6.6, 1 mM DETAPAC, 1 mM DTT, and 10% glycerol) containing 2.5 µg (5 mU) of purified E. coli DAG kinase (Calbiochem) was then added. The reaction was initiated by the addition of 5 µl of a solution containing 5 mM "cold" ATP and 0.1 µCi [γ-32P]ATP (prepared in enzyme buffer from stock solutions of 0.4 M cold ATP and 10 µCi/µl [γ-32P]ATP). Thus, the final 50 µl reaction mixture contained 0.5 mM ATP and 0.01 µCi [γ-32P] ATP. The reaction was incubated at 25ºC in a water bath for 1 hour and 5 µl was then removed and spotted onto a TLC plate and dried using a hair dryer. The phosphorylated ceramide and DAG were separated by TLC using chloroform:acetone:methanol:acetic acid:dH20 (at a volume ratio of 10:4:3:2:1) as a running solution. The ceramide phosphate signal was visualized and quantified using a Storm 860 phosphor-imager (Molecular Dyanamics, Sunnyvale, CA). Two C-18 ceramide standards (10 pmol and 100 pmol) were run on each plate for quantification of the ceramide content in the samples. For quantification, the density of the bands was analyzed using the NIH ImageJ Software.

Quantification of sphingosine-1-phosphate

S1P quantification was performed according to a recently published method [26]. Briefly, lipids were extracted from 25 µl of cell lysates by mixing with 150 µl of chloroform:methanol (1:2, v/v) and sonicated for 5 min. 100 µl each of 1 M NaCl and additional chloroform, and 10 µl of HCl (concentrated) were added. After vortexing thoroughly and centrifuging at full-speed for 2 minutes, the lower organic phase was transferred to a new tube, dried with a SpeedVac Concentrator, and resuspended in 25 µl of ethanol.

For S1P quantification, 10 µl of the lipid extraction in ethanol was added into 20 µl of the NDA derivatization reaction mixture (25 mM borate buffer, pH 9.0, containing 2.5 mM each of NDA and NaCN). The reaction mixture was diluted 1:3 with ethanol and centrifuged (13,000xg for 5 min) after incubation at 50ºC for 10 min. Thirty µl of the supernatant was then transferred to a glass sampling vial and 5 µl was applied onto a HPLC system (Waters, Milford, MA, USA) for analysis. The fluorescent derivatives were monitored using a 474 scanning fluorescence detector (Waters, Milford, MA, USA) at the excitation wavelength of 420 nm and the emission wavelength of 483 nm. Quantification of the S1P peak was calculated from a S1P standard calibration curve established using the Waters Millennium software.

Quantification of total collagen

Total soluble collagen was quantified in lung homogenates and tissue culture medium from NIH3T3 cultures using the Sircol Collagen Assay as per the manufacturer's instructions. One hundred microliters of lung homogenates or 200 µl of culture medium were incubated with 1.0 ml Sircol dye reagent. Mouse collagen was used to prepare a standard curve.

In vitro bleomycin studies

NIH3T3 cells were cultured in DMEM with 10% fetal bovine serum, 50 mU penicillin, and 50 mg streptomycin. One day before the experiment, either 30,000 cells/well were cultured in 12-well plates or, in some cases, 80,000 cells/well were cultured in 6-well plates. Bleomycin was added at a concentration of 10 µg/ml in medium containing 1% fetal bovine serum for a period of 18 or 24 hours. Cells were trypsinized, lysed by freezing/thawing and centrifuged at top speed for 10 minutes to recover supernatants for analysis.

siRNA transfection studies

NIH3T3 cells were plated in 12-well cultures dishes at a density of 40,000 cells/ml (approximately 50-60% confluent) in antibiotic-free DMEM/20% serum one day prior to transfection. Transfections were carried out as suggested by the manufacturer's instructions for use of the Lipofectamine 2000 transfection reagent (Invitrogen, Carlsbad, CA). A pool of 4 murine ASM siRNAs (50 mM final concentration) per

transfection was used (ON-TARGETplus SMARTpool duplex 9, 10, 11, and 12 for SMPD1 siRNAs from Dharmacon, Lafayette, CO). As controls, mock transfections (no siRNA) and transfections with negative control siRNA (Non-Targeting siRNA #2 D-001210-02-20 from Dharmacon) were carried out concurrently.

For each transfection sample, 2 µl containing 20 mM of murine ASM siRNA was diluted in 98 µl of Opti-MEM I reduced serum medium (Invitrogen, Carlsbad, CA), mixed gently and incubated for 5 minutes. Concurrently, 4 µl of Lipofectamine 2000 was gently mixed with 96 µl of Opti-Mem I. After 5 minutes, the siRNA was mixed with the diluted Lipofectamine and incubated for another 20 minutes at room temperature. Subsequently, the siRNA-Lipofectamine mixture (200 µl total) was added to individual wells containing the cells and medium. The plate was gently rocked back and forth for mixing and incubated at 37ºC in a CO2 incubator for at least 6 hours. The medium was replaced with fresh complete growth medium and incubated further for a total of 48 hours. For experiments with bleomycin, transfected cells were cultured for 30 hrs in DMEM/20% FBS and then the medium was replaced with DMEM/1 % FBS containing 10 ug/ml of bleomycin sulfate for another 18 hrs.

ASM expression in transfected cells

Expression of the ASM mRNA was determined by reverse-transcription polymerase chain reaction (RT-PCR), and ASM activity was measured for confirmation of reduced ASM gene expression. For determination of gene expression, RNA was isolated from transfected cells using the RNeasy Mini Kit (Qiagen, Valencia, CA) 48 hours after transfection. Briefly, cell culture medium was aspirated from the wells and the cells were washed with PBS. After complete removal of PBS, cells were detached with trypsin; serum-containing medium was added and transferred to a microcentrifuge tube. After centrifugation for 5 minutes, the supernatant was completely removed and the pellet was disrupted by addition of 600 µl Buffer RLT. The sample was homogenized by pipeting onto a QIAshredder spin column (Qiagen, Valencia, CA) and centrifuged at top speed for 2 minutes. The remainder of the procedure was carried out as per the manufacturer's instructions.

The total RNA samples were used to prepare cDNA for RT-PCR using the Superscript II kit (Invitrogen, Carlsbad, CA). The ASM gene was amplified using the following primers: 5'-AGC CGT GTC CTC TTC CTT AC-3' and 5'-CGA GAC TGT TGC CAG ACA TC-3' and the PCR conditions previously described [17]. For comparison, the murine 18sRNA gene was also amplified in each sample. The primers used in this case were: 5'-GTA ACC CGT TGA ACC CCA TT-3' and 5'-CCA TCC AAT CGG TAG TAG CG-3'.

Statistical analyses

The data were calculated as the mean ± standard error of the mean, where statistical significance was determined by the Student's t test with unequal variance or one-way ANOVA and the Tukey's Multiple Comparison Test using GraphPad Prism version 4.03 for Windows (GraphPad Software, San Diego, CA). A P-value of 0.05 or less was considered statistically significant.

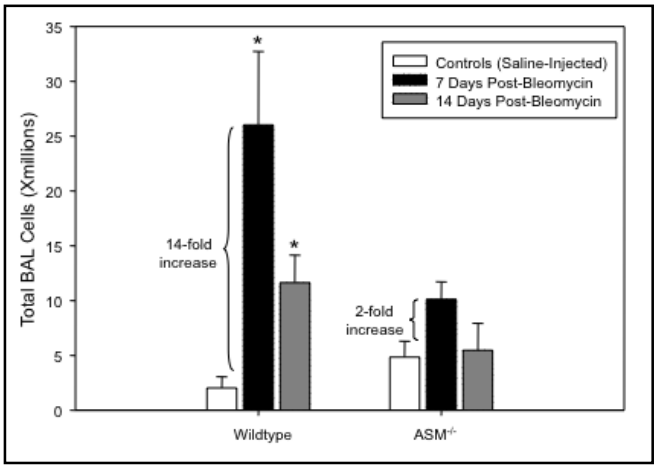

Fig. 1. The total number of inflammatory cells recovered from the pulmonary airspaces of 8-10 week old wildtype and ASM$^{-/-}$ mice by bronchoalveolar lavage (n=10 per group). By 7 days after bleomycin instillation, the numbers of cells in the lungs of wildtype mice increased 14-fold and remain significantly elevated at 14 days. In ASM$^{-/-}$ mice, the total cells in the airspaces were only elevated ~2-fold and returned to pre-bleomycin levels by 14 days. *indicates the statistically significant increase (p-value < 0.05) in bleomycin-treated wildetype animals as compared with controls (saline injected).

All cell culture experiments were performed at least in triplicate. Significant differences are indicated by a * in the figures, and the ± standard error of the mean are indicated by bars.

Results

ASM$^{-/-}$ mice exhibit an attenuated response to bleomycin treatment

We have previously shown that as ASM$^{-/-}$ mice age they accumulate increasing numbers of inflammatory cells in their pulmonary airspaces [18], beginning at ~2 months. Despite this abnormality, however, they develop no significant damage to the lung architecture within their shortened lifespans (8-10 months), other than occasional thickening of the alveolar walls [18]. As shown in Fig. 1, instillation of bleomycin into 8-10 week old ASM$^{-/-}$ mice resulted in a dramatically attenuated and insignificant inflammatory response (less than 2-fold increase versus saline controls; p=0.22), as compared to wildtype mice (greater than 14-fold increase in the bleomycin treated versus saline groups; p<0.05). At baseline (8-10 wks) there was a modest, but insignificant, increase in the total number of cells obtained from bronchoalveolar lavage of the ASM$^{-/-}$ mice, consistent with our previous observations. By 14 days post-bleomycin the inflammatory response was substantially reduced in the wildtype

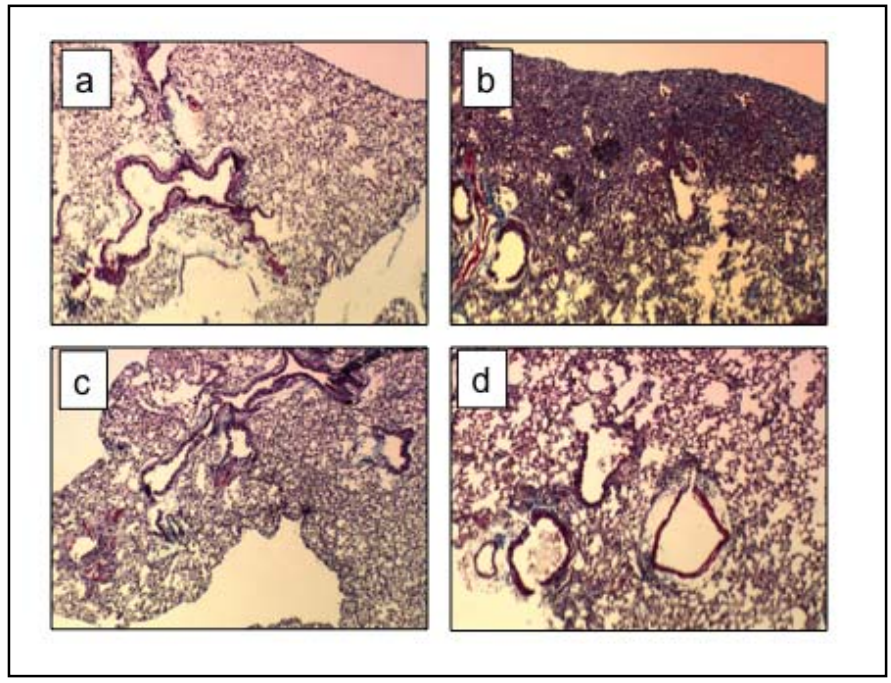

Fig. 2. Histological assessment of lungs 14 days after bleomycin exposure. Significant fibrosis is observed in lung parenchyma of bleomycin-exposed wildtype mice (b) compared with saline-treated wildtype mice (a). The lungs of ASM$^{-/-}$ mice after bleomycin exposure (d) were similar to the lungs of saline-treated counterparts (c). Lungs were stained with Trichrome. Images are shown at 40X magnification. Sections from 6 animals/group were analyzed. Representative images are shown.

animals, but remained above background (~6-fold; $p<0.05$).

Notably, H & E staining revealed only very mild fibrosis in the lungs of the treated ASM$^{-/-}$ mice at 14 days post-bleomycin, as compared with wildtype mice that exhibited extensive parenchymal fibrosis (Fig. 2, panels b & d). This was consistent with the reduced inflammatory response in the ASM$^{-/-}$ animals, and in agreement with prior literature showing that a key feature of the bleomycin fibrosis model is an early inflammatory response [27].

Trichrome staining of lung sections also showed extensive collagen deposition in fibrotic areas of bleomycin-treated wildtype mouse lungs at 14 days, and these deposits were clearly lacking in the lungs of treated ASM$^{-/-}$ mice (Fig. 3A). This observation was supported by the demonstration of a less than two-fold increase in total lung collagen after bleomycin exposure in ASM$^{-/-}$ mice ($p=0.19$), compared with an over five-fold increase in wildtype mice ($p<0.05$) (Fig. 3B). Note that ASM$^{-/-}$ mice had a modest, but insignificant, increased baseline level of total collagen in their lungs. Overall, these findings demonstrated that ASM deficiency in mice provided "protection" against the bleomycin-mediated fibrotic response.

Changes in ASM, AC and ceramide following bleomycin treatment of mouse lungs

Since ASM$^{-/-}$ mice are resistant to radiation and other forms of stress-induced apoptosis [7, 8], and in recent

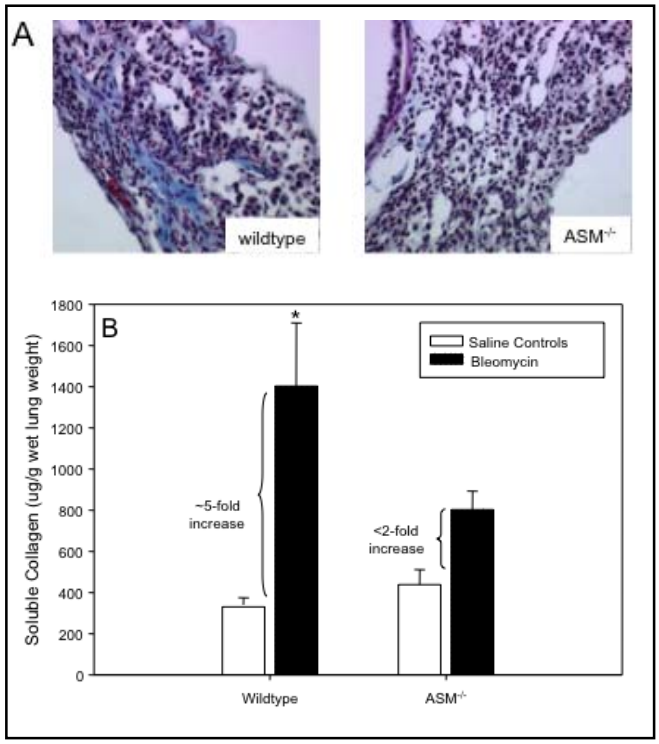

Fig. 3. Extracellular matrix deposition in bleomycin-instilled lungs. Trichrome staining (blue) highlights areas of excessive collagen deposition at fibrotic lesions seen in wildtype mice after bleomycin treatment that were not evident in ASM$^{-/-}$ mice (A). Total soluble collagen measured in whole lungs was increased ~5-fold in wildtype mice 14 days after bleomycin instillation and less than 2-fold in ASM$^{-/-}$ mice compared with their saline-treated counterparts (B). * indicates the statistically significant increase in wildtype animals compared with saline controls with a p-value < 0.05. n=10 per group.

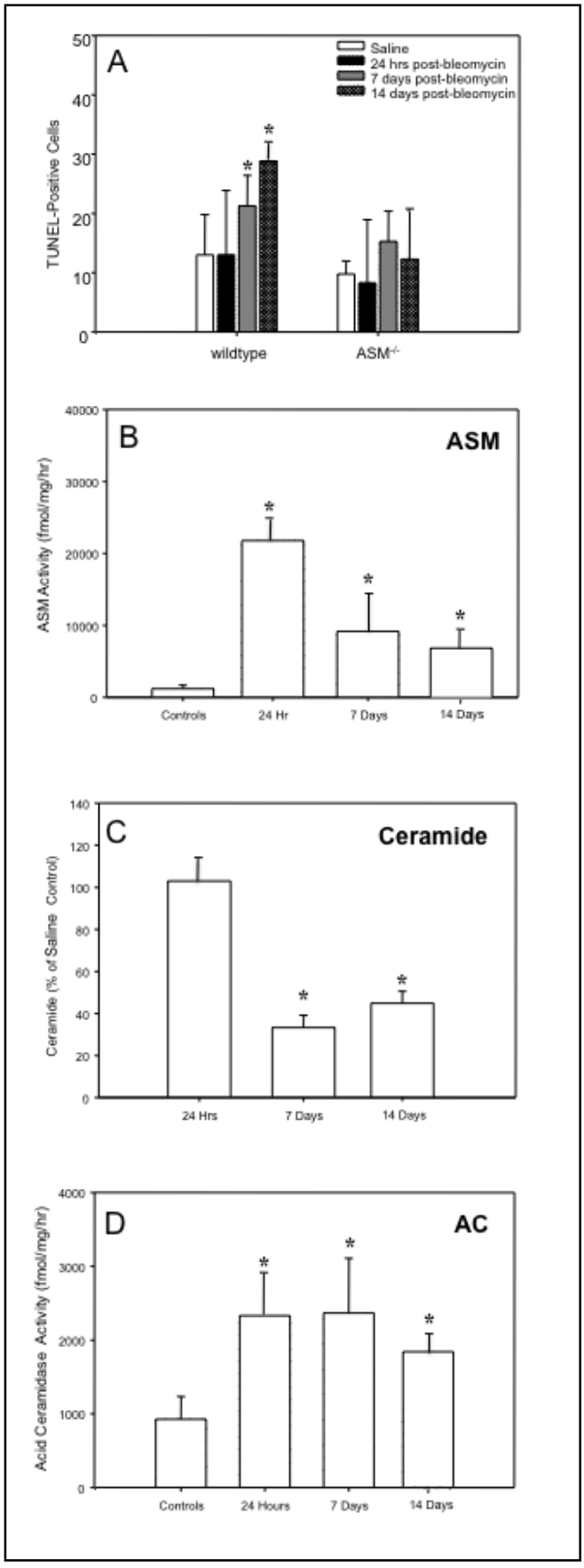

Fig. 4. The sphingomyelin/ceramide apoptosis pathway in bleomycin-instilled lungs. The numbers of TUNEL positive lung cells were significantly increased in wildtype mice starting at 7 days post-bleomycin treatment, whereas there was no significant change in the numbers of apoptotic cells in $ASM^{-/-}$ mouse lungs (A). Sections from 6 animals/group were analyzed. Representative images are shown. ASM activity also was significantly elevated in wildtype mice 24 hrs after bleomycin instillation and while reduced by 7 and 14 days, remained significantly higher than control (saline injected) mice (B). The ceramide levels in the lungs of bleomycin-treated wildtype mice were equivalent to the saline-injected controls at 24 hr, and at 7 and 14 days were significantly reduced compared with saline-treated controls (C). The acid ceramidase (AC) activity in wildtype lungs was increased at 24 hr and remained significantly elevated for up to 14 days (D). * indicates significant differences from control (saline-injected) and bleomycin-treated animals (p value <0.05).

years apoptosis has been studied as an important factor in the pathogenesis of IPF [28], we examined the *in vivo* susceptibility of lung epithelial cells to apoptosis following bleomycin exposure. In wildtype mice, the number of apoptotic cells significantly increased ($p<0.05$) over a 14 day period after bleomycin treatment, as determined by TUNEL (Fig. 4A) and Annexin V staining (unpublished data). In contrast, $ASM^{-/-}$ mice had no significant change in the numbers of apoptotic lung cells.

We next measured ASM activity in wildtype mouse lungs after bleomycin instillation, and found that it was markedly increased within 24 hr compared with saline injected mice (>10-fold; $p<0.06$) (Fig. 4B), and remained elevated at days 7 and 14 (~4-fold; $p<0.05$). Surprisingly, however, despite high ASM activity we did not observe an increase in ceramide at 24 hr post-bleomycin treatment, and in fact found that ceramide levels declined below baseline over time (Fig. 4C, $p<0.05$). We therefore hypothesized that the bleomycin treatment might also be activating other enzymes in the sphingolipid pathway that hydrolyze or modify ceramide, and determined the activity of AC, which is known to interact closely with ASM [11]. As shown in Fig. 4D, we found significant increases in this activity after bleomycin treatment of normal animals at 24 hr that were sustained for at least 14 days. Thus, elevated AC activity may explain the reduction in ceramide we observed over time following bleomycin treatment.

Alpha-smooth muscle actin-expressing fibroblasts

The appearance and proliferation of myofibroblasts at fibroblastic foci is a well-established feature of the

Fig. 5. (A) Alpha-smooth muscle actin (SMA)-expressing cells were increased in the parenchyma of lungs of wildtype mice 14 days after bleomycin exposure (e.g., b, arrow showing brown staining), but not in ASM$^{-/-}$ mice (d). As expected, both wildtype (a) and ASM-deficient (c) saline-treated control mice showed alpha-SMA expression only in smooth muscle cells around blood vessels, and not in the parenchyma. Sections from 6 animals/group were analyzed. Representative images are shown. (B) NIH3T3 fibroblasts exposed to bleomycin for 24 hours showed a marked increase in alpha-SMA expression as assessed by immunohistochemistry (black arrows point to intensely-staining cells within the cell body). There was a concomitant increase in ASM activity in NIH3T3 fibroblasts after exposure to bleomycin for 24 hr (C) and, at the same time a significant increase in collagen secretion (D). * indicates significant differences between control (saline injected) and bleomycin treated mice with a p-value <0.05.

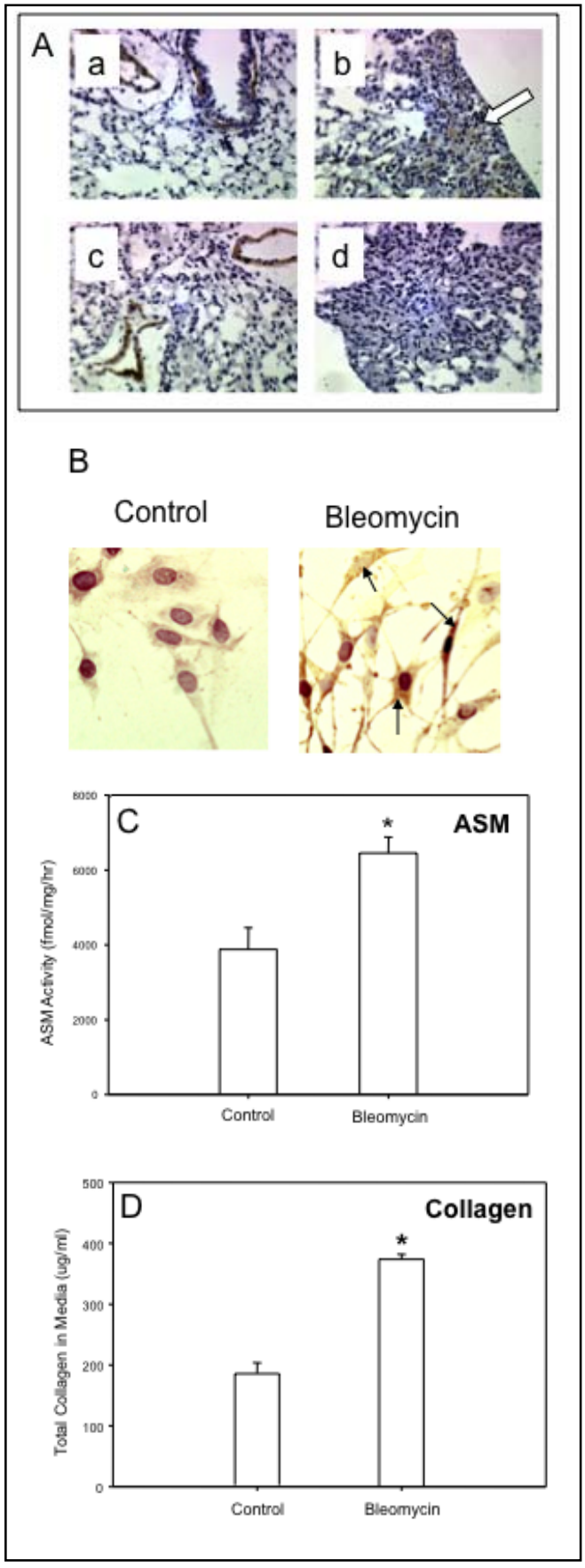

bleomycin model of pulmonary fibrosis [19-22, 29]. We found that such alpha-smooth muscle actin (alpha-SMA)-expressing cells were abundant in areas of collagen deposition within the parenchyma of lungs of wildtype mice after bleomycin exposure, in contrast to lungs from ASM$^{-/-}$ mice (Fig. 5A, panels b and d). As expected, without bleomycin treatment alpha-SMA positive smooth muscle cells were only observed surrounding blood vessels (Fig. 5A, panels a and c).

As noted above, since ASM$^{-/-}$ mice did not exhibit an inflammatory response following bleomycin exposure (Fig. 1), we could not conclude from these *in vivo* studies whether the reduced collagen deposition and lack of alpha-SMA positive foci we observed was due to attenuated inflammation, or a direct effect of ASM deficiency on fibroblast proliferation. To address this issue we next investigated the effects of bleomycin on mouse NIH3T3 fibroblasts, and found that by 24 hrs post-treatment the number of alpha-SMA-expressing fibroblasts (i.e. myofibroblasts) in the cultures was increased (Fig. 5B). ASM activity also was significantly increased in NIH3T3 fibroblasts exposed to bleomycin for 24 hrs, and there was a concomitant and significant ($p<0.05$) increase in collagen secretion into the media (Fig. 5C, D respectively).

Next, we treated the NIH3T3 cells with ASM siRNA, which significantly (almost 10-fold; $p<0.05$) reduced endogenous ASM activity as compared to mock or siNeg transfected cells (Fig. 6A, white bars). siASM transfection also significantly prevented the increase in

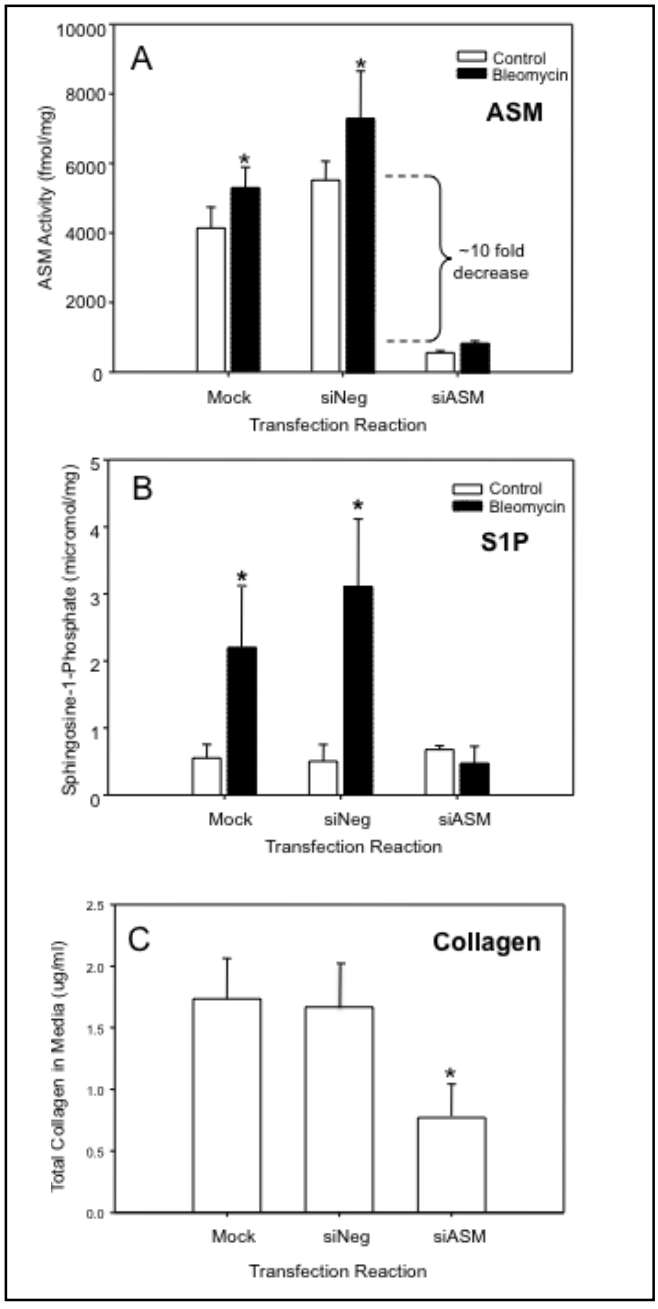

Fig. 6. ASM siRNA transfection significantly reduced endogenous ASM activity in NIH3T3 fibroblasts (A, white boxes) compared to mock and Negative (siNeg) transfected cells, and prevented the bleomycin-induced increase in this activity (A, black boxes). ASM siRNA transfection also significantly prevented the bleomycin-induced increases in sphingosine-1-phosphate (S1P) levels in these cells (B). The release of collagen also was reduced in cells transfected with ASM siRNA, in comparison with mock and siNeg-transfected cells (C). Note that due to the siRNA transfection assay, the number of cells used to detect collagen secretion in these experiments was significantly smaller than that used in Figure 5D, explaining the differences in the total collagen determined. * indicates significant differences (p-value of <0.05). Each experiment was replicated at least three times.

ASM activity we observed following bleomycin treatment (Fig. 6A, black bars), and similarly prevented the elevation of AC activity (not shown), consistent with the *in vivo* findings described above. Importantly, we also found that following bleomycin treatment of mock or siNeg transfected NIH3T3 cells there was a very significant increase in the levels of a downstream ceramide metabolite S1P, and this could be prevented by siASM transfection as well (Fig. 6B). Since S1P has a potent proliferative effect on many cell types, we hypothesized that it may, in part, be responsible for the downstream effects of ASM/AC activation we observed in wildtype mice treated with bleomycin (e.g., more alpha-SMA-positive myofibroblasts and elevated collagen; Fig. 5). Indeed, treatment of NIH3T3 cells with ASM siRNA significantly reduced ($p<0.05$) the secretion of collagen in these cultures following bleomycin exposure, compared with mock and negative siRNA transfections (Fig. 6C).

Discussion

The pathogenesis of IPF has been extensively studied and numerous factors have been implicated in this process, both in animal models and human patients [1, 3, 4, 30-34]. The complexity of factors involved is evident by the presence of both an inflammatory response and an aberrant tissue repair/remodeling process. Various cell types including inflammatory cells, epithelial cells, and fibroblasts have been shown to contribute to the overall resultant lung injury. Numerous signal transduction pathways also have been studied in the context of lung fibrosis, but ours is the first to use a specific mouse model of lung fibrosis to investigate the sphingomyelin/ceramide pathway. The data we present clearly shows that in a bleomycin-mediated model of pulmonary fibrosis ASM deficiency attenuates the development of disease. There were far fewer fibrotic lesions evident in the lungs of bleomycin-treated $ASM^{-/-}$ mice, and the quantity of extracellular matrix deposition in these areas was much less than in the abundant fibrotic lesions seen in bleomycin-treated wildtype mice, as assessed by histological analysis and measurement of total lung collagen.

Importantly, differences in the early inflammatory response between $ASM^{-/-}$ and wildtype mice also were very notable. We have previously described chronic pulmonary inflammation in $ASM^{-/-}$ mice that begins by an early age and progresses during their 8-10 month lifespan [17, 18]. Consistent with these findings, the young (8-10

week old) ASM$^{-/-}$ mice used in this study had modestly more inflammatory cells in their lungs at baseline as compared with wildtype mice. Despite this, however, bleomycin exposure resulted in only a very mild increase in the total number of inflammatory lung cells in the ASM$^{-/-}$ animals, and this was completely resolved by 14 days. This is in stark contrast to the dramatic and sustained increase in inflammatory lung cells in wildtype mice, a change that is a recognized feature of the bleomycin model [21, 22, 27] and is also identified in human IPF [1]. In the future it will be of interest to study the specific inflammatory cell type(s) that are affected by ASM, as well as the effects on cytokine/chemokine release.

Many studies have suggested that attenuation of pulmonary inflammation prevents or reduces the ultimate fibrotic outcome [22], although the true impact it may have on the fibrotic process remains unclear. Of note, corticosteroid treatment in IPF patients has proven to be largely ineffective for treating disease symptoms and causes no improvement in disease prognosis [35]. An important question raised by our findings is whether the attenuated inflammatory response in the ASM$^{-/-}$ mice was responsible for the reduced fibrosis, or if this was a more direct effect of the enzyme deficiency itself. To address this question we examined NIH3T3 cells, and found that similar to what was observed *in vivo*, bleomycin enhanced ASM expression and collagen release. Importantly, transfection of these cells with ASM siRNA prevented the collagen secretion and expression of alpha-smooth muscle actin (SMA), a marker of differentiation into myofibroblasts (unpublished data). These findings suggested that the *in vivo* observations were, at least in part, independent of inflammation.

This conclusion is supported by recent data using a carbon tetrachloride model of liver fibrosis showing that ASM is critical for the proteolytic processing of cathepsins B and D, which in turn exacerbates *in vivo* fibrosis [16]. Interestingly, liver fibrosis was reduced in ASM$^{-/-}$ mice compared to wildtype animals following carbon tetracholoride administration or bile duct ligation. ASM siRNA treatment also blunted cathepsin B and D processing in mouse and human hepatic stellate cells (LX2 cells), and prevented their activation and proliferation.

In recent years apoptosis also has emerged as an important factor in the pathogenesis of IPF [28, 32, 36]. Injury to alveolar epithelial cells and subsequent apoptosis is believed to be an important initiating event in fibrogenesis, and has been documented in both human IPF lungs and animal models of fibrosis [28, 30]. Interference with apoptotic pathways also prevented lipopolysaccharide-induced lung injury and attenuated bleomycin-mediated fibrosis in mice [31, 32, 36]. Our data shows that the numbers of apoptotic lung epithelial cells of wildtype mice were significantly increased within 14 days after bleomycin treatment, while there was no increase in apoptosis in ASM$^{-/-}$ mice (Fig. 4A). It has previously been shown that lung cells in ASM$^{-/-}$ mice are resistant to apoptosis induced by radiation and certain bacterial infections [7, 8, 37], consistent with the fact that bleomycin-induced apoptosis also was attenuated in these animals.

Apoptosis may play both a positive and a negative role in fibrogenesis. Removal of unwanted cells by the apoptotic mechanism is conducive to resolving inflammation and allowing the initiation of the repair processes, but excessive apoptosis can result in permanent damage to the pulmonary interstitium [33]. Damage to epithelial and endothelial cells creates gaps in the basement membranes, allowing the migration of fibroblasts into the alveoli and subsequently within the interstitium, ultimately resulting in remodeling of the extracellular matrix. Apoptotic cells also release cytokines and other inflammatory mediators, thereby exacerbating inflammation. The inability of bleomycin to instigate apoptosis of pulmonary cells in ASM$^{-/-}$ mice may be a contributing factor to their apparent resistance to the development of fibrosis. In the future it will be important to further characterize the lung cell types that are resistant to apoptosis in the ASM$^{-/-}$ mice.

Our data also clearly shows that bleomycin treatment caused a modulation of the sphingomyelin/ceramide pathway in wildtype mice. ASM activity was markedly increased starting at 24 hours and remained significantly higher than background for up to 14 days. Acid ceramidase activities also were increased, perhaps explaining why the ceramide levels in lung tissue were not elevated and, in fact, decreased over time. Acid ceramidase is one of several ceramidases that can degrade ceramide, thereby producing the lipid sphingosine, which is rapidly converted to S1P by the action of sphingosine kinases. Although we did not measure sphingosine and S1P in the lung tissues of bleomycin treated animals, we did find that bleomycin treatment of NIH3T3 cells led to an increase in S1P, which is consistent with elevated AC. Interestingly, it has been shown that the S1P/S1P1 receptor pathway is an important regulator of vascular permeability, a key feature leading to tissue injury [38]. However, given that the blood levels of S1P are normally quite high, it is not generally thought that S1P induces fibrosis. This raises the interesting possibility

that sphingosine may be eliciting the fibrotic response following bleomycin treatment, rather than S1P. The role of sphingosine in lung injury has not been studied in detail, but could be the subject of interesting, future investigations. Moreover, it is also possible that ceramide produced by AC could be converted to ceramide-1-phosphate, thereby activating phospholipase A2 and triggering inflammation and fibrosis.

An intriguing feature of the bleomycin response in $ASM^{-/-}$ mice was the virtual lack of myofibroblasts in the pulmonary interstitium of these animals. Myofibroblasts are defined as SMA-expressing cells that are capable of collagen secretion. The presence of these activated cells at sites of tissue repair and subsequent tissue damage is believed to be imperative in fibrosis, and was abundantly seen in areas of excessive collagen deposition in wildtype mice treated by bleomycin (Fig. 5A). The origin of these cells is unknown, but one possible mechanism is the activation of fibroblasts by TGFbeta-mediated differentiation or via some other cellular mediators [34]. There is growing evidence showing that ceramide and S1P play important roles in cellular differentiation via TGFbeta mediation [39], and the specific role of this protein in the bleomycin-response of $ASM^{-/-}$ mice also requires further investigation. Of note, we have previously shown that TGFbeta levels are not elevated in these mice, despite marked inflammation [18].

In order to determine the effect of ASM deficiency on fibroblasts in isolation from possible influences of the pulmonary milieu, including inflammation, we used NIH3T3 cells exposed to bleomycin in culture. Bleomycin treatment led to an increase in ASM activity and collagen release, indicating that differentiation had occurred (Fig. 5C and D). Importantly, when ASM activity was significantly reduced in the fibroblasts by siRNA treatment, collagen secretion also was reduced to normal. We also examined alpha-SMA expression in the transfected cells, and despite high background levels of this protein due to the high serum conditions required for transfection, a clear reduction was observed in siASM treated compared to control cells (unpublished data).

Thus, these cell culture data suggest that the protective effect against bleomycin observed in the $ASM^{-/-}$ mice was not due to an attenuated inflammatory response alone. The findings also suggests that S1P may be an important contributing factor to IPF leading to myofibroblast differentiation, and that the S1P may be derived, at least in part, from elevated AC. It is important to note that the only known mechanism to produce sphingosine, the precursor of S1P, is via the hydrolysis of ceramide by ceramidases. Work by others also has shown that an analogue of S1P induces differentiation of fibroblasts into myofibroblasts *in vitro* [40], lending credence to this hypothesis.

Together, these data imply an important role for both ASM and AC in myofibroblast differentiation/activation, and in the development of bleomycin-mediated fibrosis. In the future it will be interesting to further explore the role of S1P by using mice in which specific S1P receptors have been inactivated, and/or by modulation of sphingosine kinases, the enzymes responsible for S1P production. It would also be interesting to examine the occurrence of IPF in patients with Types A and B Niemann-Pick disease, who have inherited deficiencies in ASM activity, as well as in patients with Farber disease, the genetic disorder of AC deficiency. However, these are extremely rare genetic disorders, and controlled clinical studies of this nature will be very difficult to carryout. Conversely, examination of the sphingolipid signaling molecules in the lungs of patients with IPF also would be of interest.

Clearly, fibrogenesis is a complex process and many studies aimed at identifying targets for the treatment of IPF are ongoing [2, 35]. As noted above, targeting inflammation alone has largely proven to be ineffective, and the search for other potential processes involved in the fibrotic process are continuing. Our findings suggest that targeting factors that influence fibroblast differentiation into collagen-secreting cells may be beneficial in preventing or reducing the progressive matrix remodeling that occurs in fibrosis. Specifically, developing strategies to reduce the ASM activity in lung cells of individuals diagnosed with fibrosis deems further investigation. In this regard we have also found that mice heterozygous for the ASM knockout allele ($ASM^{+/-}$ with ~50% of ASM activity) showed some protection from bleomycin-induced lung injury (unpublished data), consistent with observations in the liver fibrosis models [16]. Moreover, cystic fibrosis mice that were heterozygous for the ASM knockout ($Cftr^{-/-}ASM^{+/-}$) had reduced pulmonary cell death and DNA deposition, and, importantly, also had normal susceptibility to *P. aeruginosa* infection [13, 14]. This suggests that in a therapeutic context complete reduction of ASM activity may not be necessary to achieve some benefits.

Our results are also in agreement with other recent reports showing that the sphingolipid signaling pathway, and ASM activation in particular, is involved in the pathogenesis of acute lung injury induced by a number of different extrinsic factors [e.g., 37, 41, 42]. It may therefore be particularly useful to target this pathway for

preventing pulmonary toxicity and the subsequent development of interstitial lung fibrosis induced by several chemotherapy drugs, including bleomycin. As noted above, bleomycin is an effective drug for several types of cancer, and reduction of associated side effects, including pulmonary fibrosis, would undoubtedly increase its benefit [43, 44]. Use of ASM inhibition in this manner also might avoid the complexity of chronic administration of an enzyme inhibitor, which may similarly have unwanted side effects.

Acknowledgements

This work was supported by a grant to EHS from the National Institutes of Health (5 R01 HD28607).

References

1 Maher TM, Wells AU, Laurent GJ: Idiopathic pulmonary fibrosis: multiple causes and multiple mechanisms? Eur Respir J 2007;30:835-839.

2 Hauber HP, Blaukovitsch M: Current and future treatment options in idiopathic pulmonary fibrosis. Inflamm Allergy Drug Targets 2010; in press.

3 Chua F, Gauldie J, Laurent GL: Pulmonary fibrosis: searching for model answers. Am J Respir Cell Mol Biol 2005;33:9-13.

4 Tager AM, LaCamera P, Shea BS, Campanella GS, Selman M, Zhao A, Polosukhin V, Wain J, Karimi-Shah B, Kim ND, Hart WK, Pardo A, Blackwell TS, Xu Y, Chun J, Luster AD: The lysophosphatidic acid receptor LPA1 links pulmonary fibrosis to lung injury by mediating fibroblast recruitment and vascular leak. Nat Med 2008;14:45-54.

5 Scotton CJ, Chambers RC: Molecular targets in pulmonary fibrosis: the myofibroblast in focus. Chest 2007;132:1311-1321.

6 Phan SH: Biology of fibroblasts and myofibroblasts. Proc Am Thorac Soc 2008;5:335-337.

7 Smith EL, Schuchman EH: The unexpected role of acid sphingomyelinase in cell death and the pathophysiology of common diseases. FASEB J 2008;22:3419-3431.

8 Jenkins RW, Canals D, Hannun YA: Roles and regulation of secretory and lysosomal acid sphingomyelinase. Cell Signal 2009;21:836-846.

9 Grassme H, Riethmuller J, Gulbins E: Biological aspects of ceramide enriched membrane domains. Prog Lipid Res 2007;46:161-170.

10 Hannun YA, Obeid, LM: Principles of bioactive lipid signaling: lessons from sphingolipids. Nat Rev Mol Cell Biol 2008;9:139-150.

11 He X, Okino N, Dhami R, Dagan A, Gatt S, Schulze H, Sandhoff K, Schuchman EH: Purification and characterization of recombinant, human acid ceramidase. Catalytic reactions and interactions with acid sphingomyelinase. J Biol Chem 2003;278:32978-32986.

12 Fyrst H, Saba JD: An update on sphingosine-1-phosphate and other sphingolipid mediators. Nat Chem Biol 2010;6:489-497.

13 Teichgraber V, Ulrich M, Endlich N, Riethmuller J, Wilker B, De Oliveria-Munding CC, van Heeckeren AM, Barr ML, von Kurthy G, Schmid KW, Weller M, Tummier B, Lang F, Grassme H, Doring G, Gulbins E: Ceramide accumulation mediates inflammation, cell death and infection susceptibility in cystic fibrosis. Nat Med 2008;14:382-391.

14 Becker KA, Riethmuller J, Luth A, Doring G, Kleuser B, Gulbins E: Acid sphingomyelinase inhibitors normalize pulmonary ceramide and inflammation in cystic fibrosis. Am J Respir Cell Mol Biol 2010;42:716-724.

15 Riethmuller J, Anthonysamy J, Serra E, Schwab M, Doring G, Gulbins E: Therapeutic efficacy and safety of amitriptyline in patients with cystic fibrosis. Cell Physiol Biochem 2009;24:65-72.

16 Moles A, Tarrats N, Morales A, Dominguez M, Bataller R, Caballeria J, Garcia-Ruiz C, Fernandez-Checa JC, Mari M: Acidic sphingomyelinase controls hepatic stellate cell activation and in vivo liver fibrosis. Am J Path 2010;177:1214-1224.

17 Horinouchi K, Erlich S, Perl DP, Ferlinz K, Bisgaier CL, Sandhoff K, Desnick RJ, Stewart CL, Schuchman EH: Acid sphingomyelinase deficient mice: a model of types A and B Niemann-Pick disease. Nat Genet 1995;10:288-293.

18 Dhami R, He X, Gordon RE, Schuchman EH: Analysis of the lung pathology and alveolar macrophage function in the acid sphingomyelinase-deficient mouse model of Niemann-Pick disease. Lab Invest 2001;81:987-999.

19 Cooper JA, White D, Matthay R: Drug-induced pulmonary disease. Am Rev Respir Dis 1986;133:321-340.

20 Sigounas G, Salleng KJ, Mehlhop PD, Sigounas DG: Erythropoiten ameliorates chemotherapy-induced fibrosis of the lungs in a preclinical murine model. Int J Cancer 2008;122:2851-2857.

21 Moore BB, Hogaboam CM: Murine models of pulmonary fibrosis. Am J Physiol Lung Cell Mol Physiol 2008;294:L152-60.

22 Moeller A, Ask K, Warburton D, Gauldie J, Kolb M: The bleomycin animal model: A useful tool to investigate treatment options for idiopathic pulmonary fibrosis? Int J Biochem Cell Biol. 2008;40:362-382.

23 He X, Chen F, Dagan A, Gatt S, Schuchman EH: A fluorescence-based, high-performance liquid chromatographic assay to determine acid sphingomyelinase activity and diagnose types A and B Niemann-Pick disease. Anal Biochem 2003;314:116-120.
24 He X, Li CM, Park JH, Dagan A, Gatt S, Schuchman EH: A fluorescence-based high-performance liquid chromatographic assay to determine acid ceramidase activity. Anal Biochem 1999;274:264-269.
25 Schneider EG, Kennedy EP: Phosphorylation of ceramide by diglyceride kinase preparations from Escherichia coli. J Biol Chem 1973;248:3739-3741.
26 He X, Huang CL, Schuchman EH: Quantitative analysis of sphingosine-1-phosphate by HPLC after naphthalene-2,3dicarboxaldehyde (NDA) derivatization. J Chromatogr B Analyt Technol Biomed Life Sci 2009;877:983-990.
27 Izbicki G, Segel MJ, Christensen TG, Conner MW, Breuer R: Time course of bleomycin-induced lung fibrosis. Int J Exp Path 2002;83:111-119.
28 Barbas-Filho JV, Ferreira MA, Sesso A, Kairalla RA, Carvalho CR, Capelozzi VL: Evidence of type II pneumocyte apoptosis in the pathogenesis of idiopathic pulmonary fibrosis (IPF)/usual interstitial pneumonia (UIP). J Clin Pathol 2001;54:132-138.
29 Powell DW, Mifflin RC, Valentich JD, Crowe SE, Saada JI, West AB: Myofibroblasts. I. Paracrine cells important in health and disease. Am J Physiol Cell Physiol 1999;277:C1-C19.
30 Kanko Y, Hara N: Induction of apoptosis and pulmonary fibrosis in mice in response to ligation of Fas antigen. Am J Respir Cell Mol Biol 1997;17:272-278.
31 Hagimoto N, Kuwano K, Miyazaki H, Kunitake R, Fujita M, Kawasaki M, Wang Q, Wang Y, Hyde DM, Gotwals PJ, Lobb RR, Ryan ST, Giri SN: Effect of antibody against integrin alpha4 on bleomycin-induced pulmonary fibrosis in mice. Biochem Pharmacol 2000;60:1949-1958.
32 Kuwano K, Kunitake R, Maeyama T, Hagimoto N, Kawasaki M, Matsuba T, Yoshimi M, Inoshima I, Yoshida K, Hara N: Attenuation of bleomycin-induced pneumopathy in mice by a caspase inhibitor. Am J Physiol Lung Cell Mol Physiol 2001;280:L316-L325.
33 Kuwano K: Involvement of epithelial cell apoptosis in interstitial lung diseases. Inter Med 2008;47:345-353.
34 Caraci F, Gili E, Calafiore M, Failla M, La Rosa C, Crimi N, Sortino MA, Nicoletti F, Copani A, Vancheri C: TGF-beta1 targets the GSK-3beta/beta-catenin pathway via ERK activation in the transition of human lung fibroblasts into myofibroblasts. Pharmacol Res 2008;57:274-282.
35 Bouros D, Antoniou KM: Current and future therapeutic approaches in idiopathic pulmonary fibrosis. Eur Respir J 2005;26;693-702.
36 Kawasaki M, Kuwano K, Hagimoto N, Matsuba T, Kunitake R, Tanaka T, Maeyama T, Hara N: Protection from lethal apoptosis in lipopolysaccharide-induced acute lung injury in mice by a caspase inhibitor. Am J Pathol 2000;157:597-603.
37 Petrache I, Natarajan V, Zhen L, Medler TR, Richter AT, Cho C, Hubbard WC, Berdyshev EV, Tuder RM: Ceramide upregulation causes pulmonary cell apoptosis and emphysema-like disease in mice. Nat Med 2005;11:491-498.
38 Shea BS, Brooks SF, Fontaine FA, Chun J, Luster AD, Tager AM: Prolonged S1P1 agonist exposure exacerbates vascular leak, fibrosis, and mortality after lung injury. Am J Respir Cell Mol Biol 2010; in press.
39 Kono Y, Nishiuma T, Nishimura Y, Kotani Y, Okada T, Nakamura S, Yokoyama M: Sphingosine kinase 1 regulates differentiation of human and mouse lung fibroblasts mediated by TGF-beta1. Am J Respir Cell Mol Biol 2007;37:395-404.
40 Keller CD, Rivera Gil P, Tolle M, van der Giet M, Chun J, Radeke HH, Schafr-Korting M, Kleuser B: Immunomodulator FTY720 induces myofibroblast differentiation via lysophospholipid receptor S1P3 and Smad3 signaling. Am J Path 2007;170:281-292.
41 Mercier JC, Dinh-Xuan AT: Neutralizing ceramide: a major breakthrough or yet another marginal target for the treatment of acute lung injury? Pediatr Res 2005;57:319-321.
42 von Bismarck P, Garcia Wistadt CF, Klemm K, Winoto-Morbach S, Uhlig U, Schutze S, Adam D, Lachmann B, Uhlig S, Krause MF: Improved pulmonary function by acid sphingomyelinase inhibition in a newborn piglet lavage model. Am J Respir Crit Care Med 2008;177:1233-1241.
43 Feldman DR, Bosl GJ, Sheinfeld J, Motzer RJ: Medical treatment of advanced testicular cancer. JAMA 2008;299:672-684.
44 Martin WG, Ristow KM, Habermann TM, Colgan JP, Witzig TE, Ansell SM: Bleomycin pulmonary toxicity has a negative impact on the outcome of patients with Hodgkin's lymphoma. J Clin Oncol 2005;23:7614-7620.